Electronic Supplementary Material (ESI) for Chemical Science.

Supporting Information

$Ir_6In_{32}S_{21}$, A polar, metal-rich semiconducting subchalcogenide

Jason F. Khoury[1], Jiangang He[2], Jonathan E. Pfluger[2], Ido Hadar[1], Mahalingam Balasubramanian[3], Constantinos C. Stoumpos[4], Rui Zu[5], Venkatraman Gopalan[5,6], Chris Wolverton[2], and Mercouri G. Kanatzidis[1*]

[1]*Department of Chemistry, Northwestern University, Evanston, Illinois 60208, United States*
[2]*Department of Materials Science and Engineering, Northwestern University, Evanston, Illinois 60208, United States*
[3]*Advanced Photon Source, Argonne National Laboratory, Argonne, Illinois 60439, USA*
[4]*Department of Materials Science and Technology, Voutes Campus, University of Crete, Heraklion GR-70013, Greece*
[5]*Materials Research Institute and Department of Materials Science and Engineering, Pennsylvania State University, 212-N MSC Building, University Park, Pennsylvania 16802, USA*
[6]*Department of Physics, Pennsylvania State University, University Park, Pennsylvania 16802, USA*

Table of Contents

Powder X-ray Diffraction. Powder x-ray diffraction (PXRD) data were taken using a Rigaku Miniflex powder x-ray diffractometer with Ni-filtered CuKα radiation (λ = 1.5406 Å) at 40 kV and 15 mA. Scan widths were 0.02° for all scans, and the scan rate was 10°/min. PXRD patterns for $Ir_6In_{32}S_{21}$ were simulated using Mercury CSD 3.8.

Scanning Electron Microscopy (SEM) and Energy Dispersive Spectroscopy (EDS). SEM and semi-quantitative EDS were performed with a Hitachi S-3400 scanning electron microscope equipped with a PGT energy-dispersive x-ray analysis attachment. Parameters for the EDS measurements were 25 kV, 70 mA probe current, and a 60 s acquisition time. EDS data were taken from several flux-grown single crystals of $Ir_6In_{32}S_{21}$ with flat, well-defined faces.

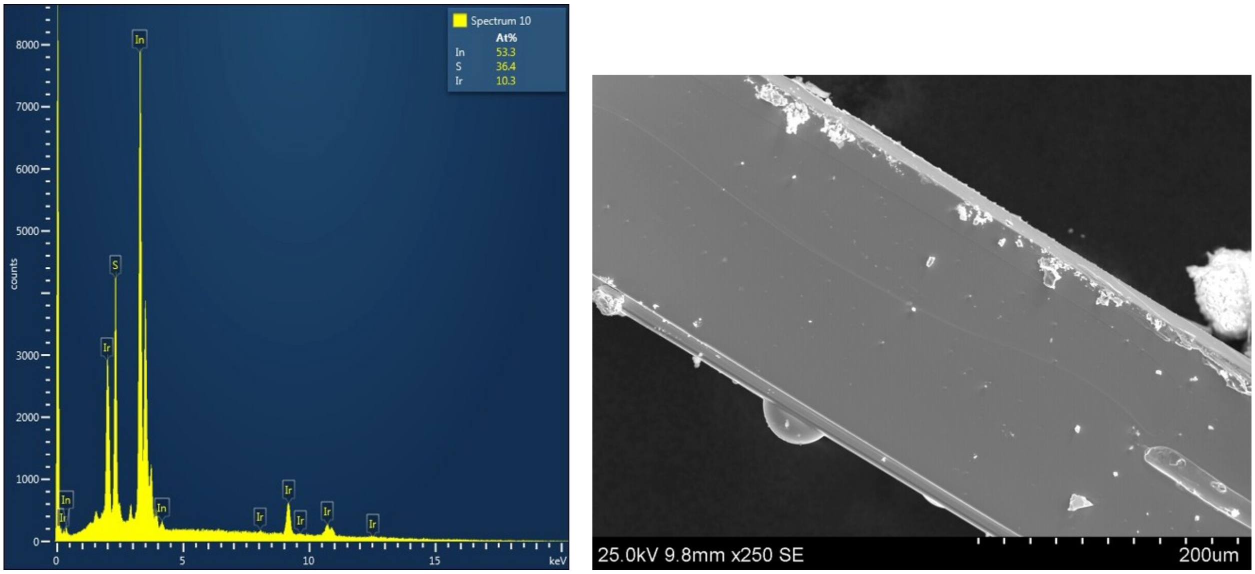

Figure S1. EDS (left) and SEM (right) for $Ir_6In_{32}S_{21}$. The average chemical composition from the EDS data is $Ir_6In_{31.0}S_{21.2}$.

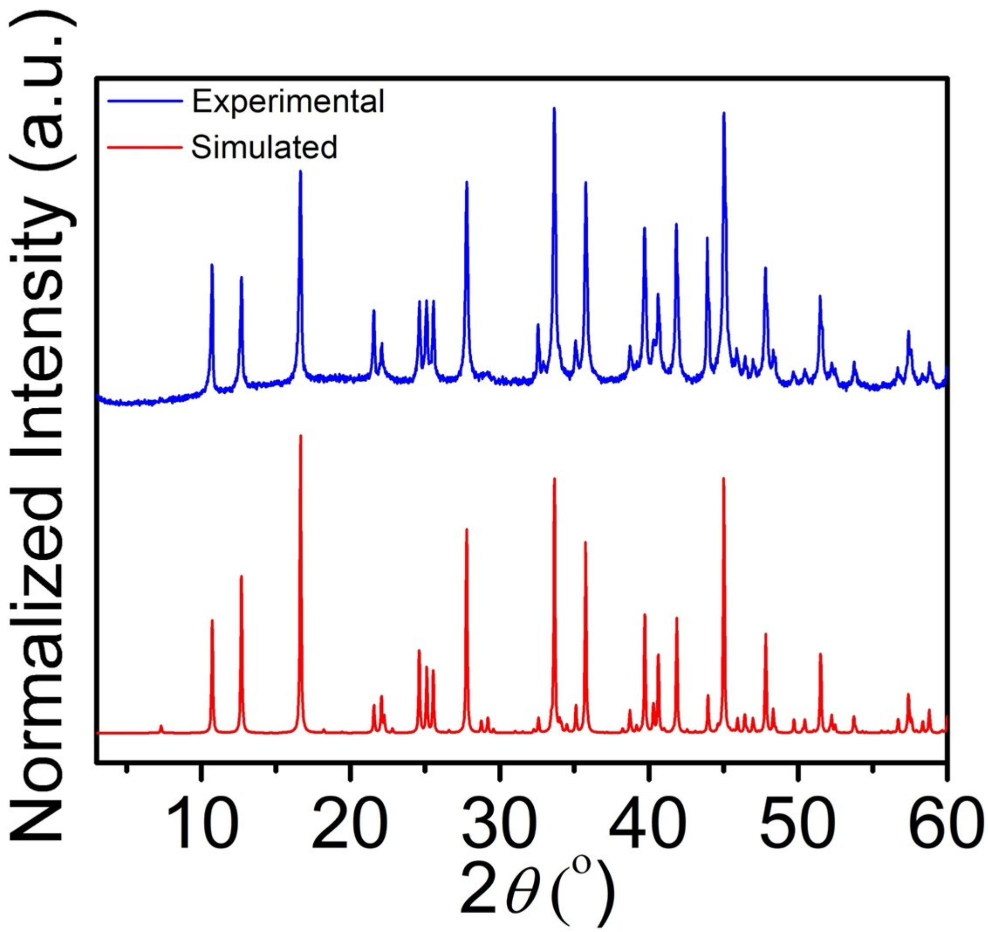

Figure S2. Experimental PXRD data of $Ir_6In_{32}S_{21}$ (top) in blue compared to its simulated diffraction pattern (bottom) in red.

SHG Polarimetry of $Ir_6In_{32}S_{21}$

Dipolar second harmonic generation (SHG), which is defined as $P_i = d_{ijk}E_jE_k$, is a characteristic of non-centrosymmetric materials and can be used as a nondestructive tool to characterize symmetry properties such as the point group of a material.[1, 2] Due to the absence of inversion symmetry in $Ir_6In_{32}S_{21}$, SHG signals of $Ir_6In_{32}S_{21}$ are observed through normal reflection geometry as shown in the Figure 3a). The polarization direction of a linear polarized light is effectively rotated by a half waveplate and focused onto the sample. The generated SHG signals are then collected as a function of polarization direction (θ) of incident beam along two orthogonal directions, [100] and [120] directions of the crystal respectively. Simulated response with point group 3*m* is also calculated to fit the experimental data to confirm the point group as well as its nonlinear optical properties with detailed equation shown below,

$$I_{[100]}^{2w}(\varphi) = \left|E_{[100]}^{2w}(\varphi)\right|^2 \propto \left|d_{22}E_0\cos(2\varphi)\right|^2$$

$$I_{[120]}^{2w}(\varphi) = \left|E_{[120]}^{2w}(\varphi)\right|^2 \propto \left|d_{22}E_0\sin(2\varphi)\right|^2$$

where E_0 is the amplitude of incident beam and E^{2w} is the generated SHG fields. Due to the geometry of the crystal, the d_{22} is the only accessible SHG coefficient through normal reflection geometry. This is because of the crystal geometry ([001] out of plane), as the electric field at 800 nm will be restricted to 1,2 directions where 1,2,3 represents crystal principle axes (1 along [100], 2 perpendicular to [100] and [001]; 3 along [001]). The d_{24} is not involved because it represents d_{223}, where E_2 and E_3 give rise to the P_2 ($P_2 = d_{223}E_2E_3$), and E_3 is 0 because there is no electric field along the propagation direction (normal reflection suggest *k*//3 direction, thus $E_3 = 0$), thus d_{24} is not involved in the expression. The applied laser with a wavelength of 800 nm was from a pulsed Ti-Sapphire femtosecond laser system (100 fs, 1 kHz). Lithium niobate was used as the reference sample for alignment.

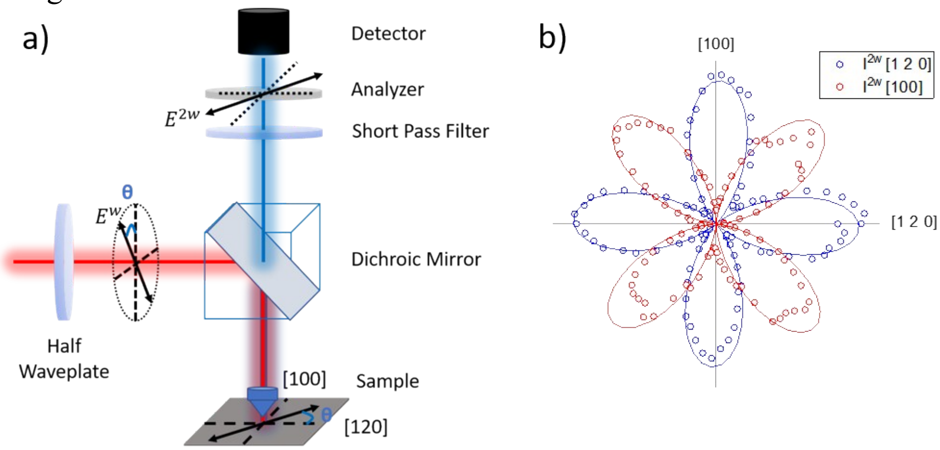

Figure S3. SHG geometry and polar plot of $Ir_6In_{32}S_{21}$. a) Schematic of experimental set up. b) SHG signals of $Ir_6In_{32}S_{21}$. The open circle represents experimental data and solid line is theoretical fitting. Blue curve represents SHG data collected along [120] direction and red represents SHG data collected along [100] direction.

Thus, SHG confirms the non-centrosymmetric properties of $Ir_6In_{32}S_{21}$. By comparing the experimental data with theoretical fitting, the simulated curve shows reasonable match with the experimental curve confirming that 3*m* is the valid point group of $Ir_6In_{32}S_{21}$.

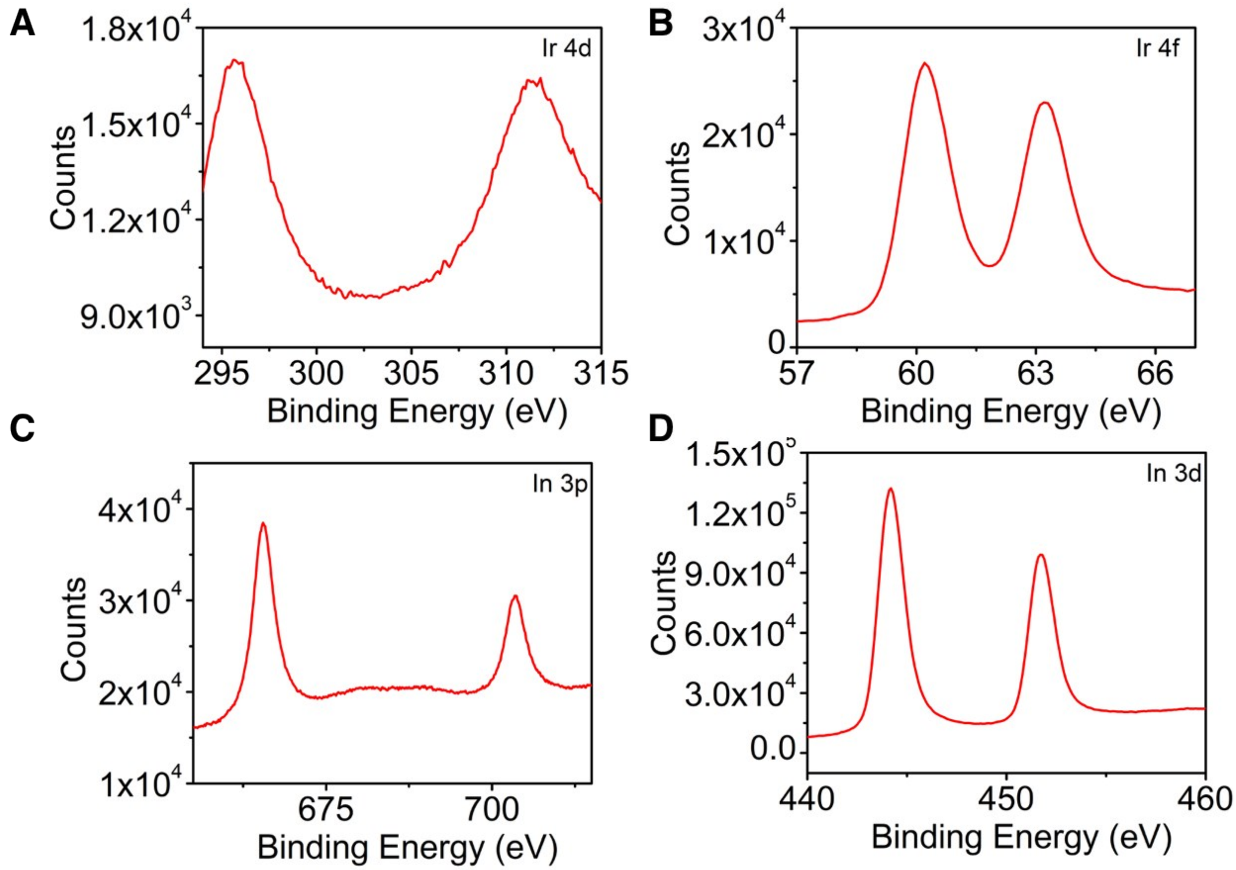

Figure S4. XPS data for Ir 4d and 4f (A, B) and In 3p and 3d (C, D).

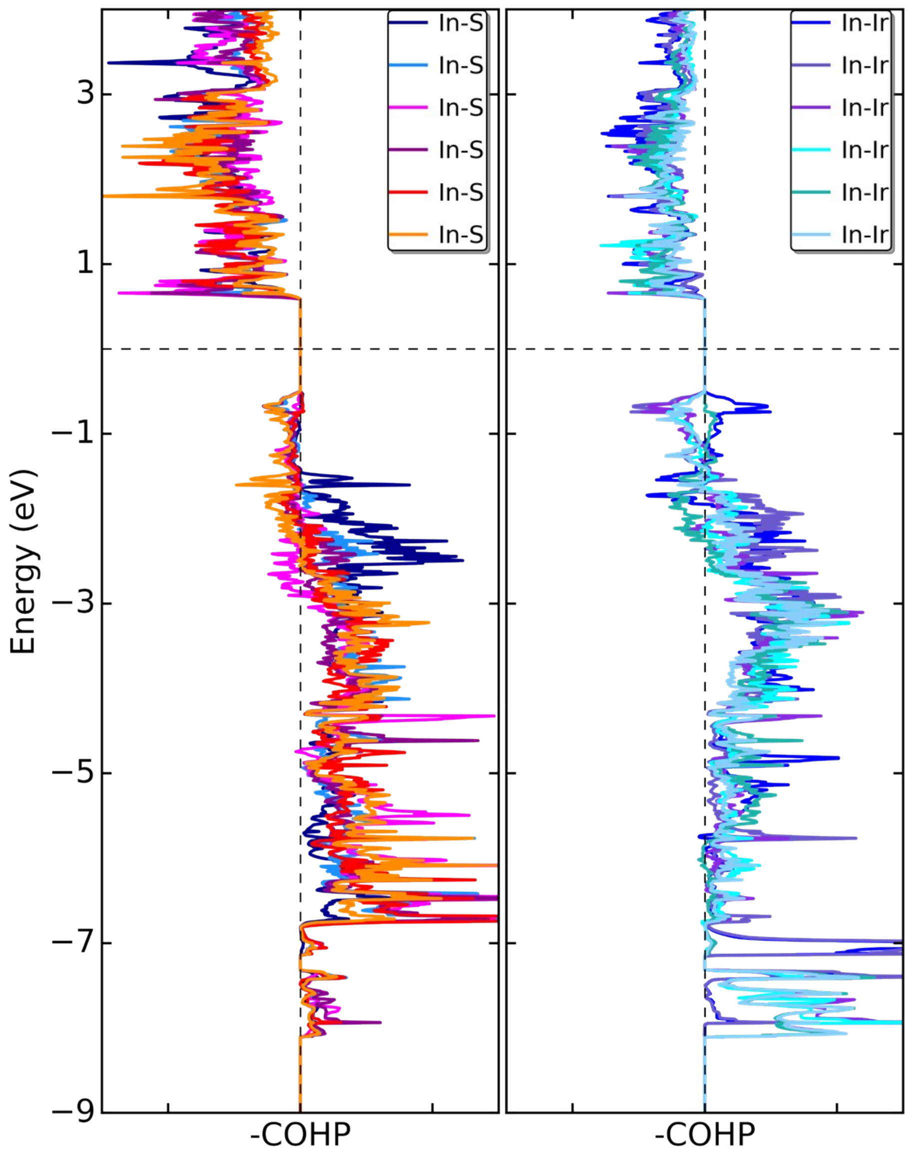

Figure S5. Additional crystal orbital Hamilton population (COHP) data of $Ir_6In_{32}S_{21}$ for the In-S (left) and Ir-In (right) interactions. The left side (negative) of the –COHP plot designates antibonding interactions, and the right side (positive) indicates bonding interactions. Both In-S and Ir-In interactions show bonding character.

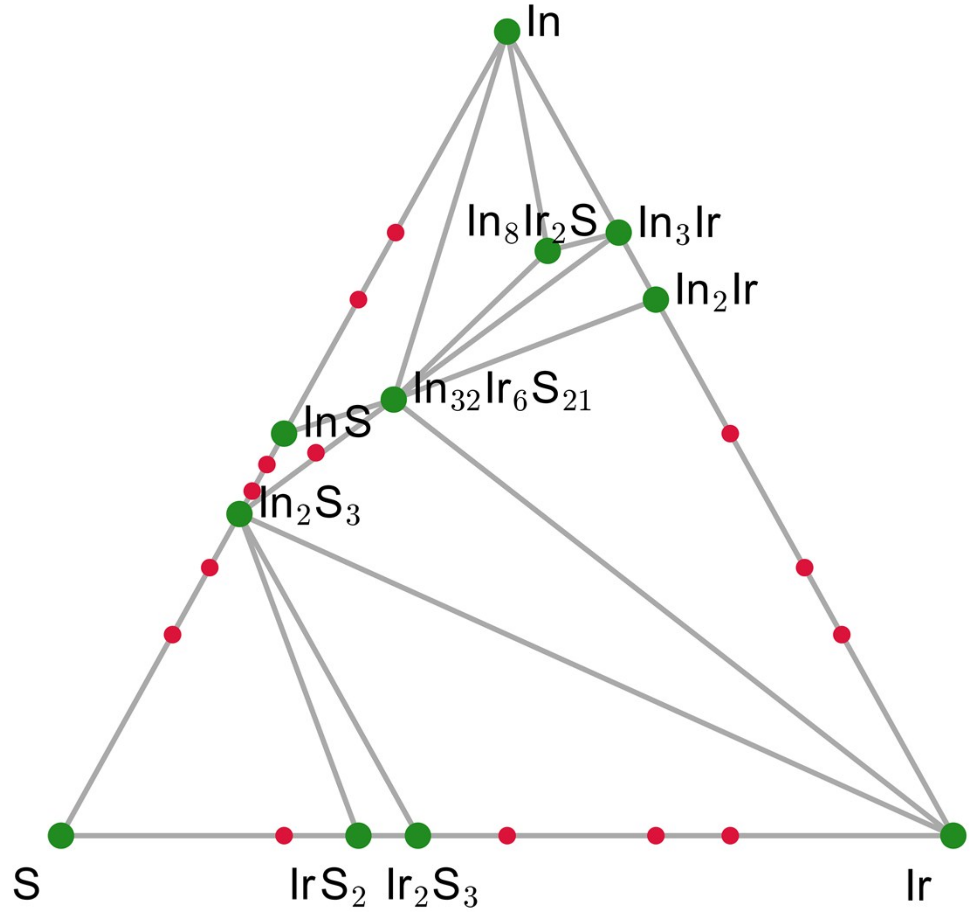

Figure S6. The 0 K phase diagram of the Ir-In-S system generated by the Open Quantum Materials Database (OQMD). The large green and small red dots indicate stable and unstable phases, respectively.

Table S1. Atomic coordinates (x10^4) and equivalent isotropic displacement parameters (Å^{2}x10^3) for $Ir_6In_{32}S_{21}$ at 299 K with estimated standard deviations in parentheses.

Label	x	y	z	Occupancy	U_{eq}*
Ir(1)	0	3342(1)	9110(1)	1	5(1)
Ir(2)	3333	6667	6383(1)	1	5(1)
Ir(3)	0	10000	6470(2)	1	6(1)
In(1)	1831(1)	8494(1)	1012(2)	1	16(1)
In(2)	0	4787(1)	1137(2)	1	18(1)
In(3)	3304(1)	4804(1)	5699(2)	1	14(1)
In(4)	0	3346(1)	5905(2)	0.95	11(1)
In(5)	1830(1)	5224(1)	8373(2)	1	18(1)
In(6)	3333	6667	3142(2)	0.95	12(1)
In(7)	1498(1)	10000	8236(2)	1	23(1)
In(8)	0	8559(2)	4552(2)	0.8	18(1)
S(1)	1554(2)	3370(2)	4176(4)	1	11(1)
S(2)	0	4921(3)	4207(5)	1	11(1)
S(3)	1838(3)	6644(2)	1072(4)	1	12(1)
S(4)	0	8428(3)	1261(6)	1	19(1)
S(5)	3410(4)	3410(4)	7525(8)	1	26(2)
In(9)	0	8236(4)	5440(9)	0.2	18(1)
In(10)	0	10000	2900(50)	0.25	142(13)

*U_{eq} is defined as one third of the trace of the orthogonalized U_{ij} tensor.

Table S2. Anisotropic displacement parameters (Å^{2}x10^3) for $Ir_6In_{32}S_{21}$ at 299 K with estimated standard deviations in parentheses.

Label	U_{11}	U_{22}	U_{33}	U_{12}	U_{13}	U_{23}
Ir(1)	4(1)	4(1)	6(1)	2(1)	0	0(1)
Ir(2)	5(1)	5(1)	5(1)	2(1)	0	0
Ir(3)	5(1)	5(1)	8(1)	3(1)	0	0
In(1)	15(1)	15(1)	20(1)	8(1)	10(1)	9(1)
In(2)	12(1)	17(1)	23(1)	6(1)	0	-13(1)
In(3)	14(1)	9(1)	20(1)	7(1)	-1(1)	-3(1)
In(4)	13(1)	13(1)	6(1)	6(1)	0	0(1)
In(5)	14(1)	13(1)	17(1)	-1(1)	5(1)	5(1)
In(6)	15(1)	15(1)	8(1)	7(1)	0	0
In(7)	17(1)	42(1)	18(1)	21(1)	-6(1)	0
In(8)	14(1)	17(1)	22(1)	7(1)	0	-13(1)
S(1)	11(2)	11(2)	10(2)	5(1)	-1(1)	-1(1)
S(2)	10(2)	11(2)	12(2)	5(1)	0	-3(2)
S(3)	12(2)	13(2)	12(2)	6(1)	1(1)	0(1)
S(4)	11(2)	17(2)	25(2)	6(1)	0	-1(2)
S(5)	28(2)	28(2)	31(3)	21(2)	13(2)	13(2)
In(9)	14(1)	17(1)	22(1)	7(1)	0	-13(1)
In(10)	116(14)	116(14)	190(40)	58(7)	0	0

The anisotropic displacement factor exponent takes the form: $-2\pi^2[h^2a^{*2}U_{11} + ... + 2hka^*b^*U_{12}]$.

Table S3. Bond lengths [Å] for $Ir_6In_{32}S_{21}$ at 299 K with estimated standard deviations in parentheses.

Label	Distances
Ir(1)-In(1)#1	2.6212(10)
Ir(1)-In(1)#2	2.6212(10)
Ir(1)-In(2)#3	2.6155(12)
Ir(1)-In(4)	2.6385(15)
Ir(1)-In(5)	2.6581(10)
Ir(1)-In(5)#4	2.6581(9)
Ir(1)-In(7)#5	2.6694(13)
Ir(2)-In(3)	2.6366(8)
Ir(2)-In(3)#5	2.6365(8)
Ir(2)-In(3)#6	2.6365(8)
Ir(2)-In(5)#6	2.6275(10)
Ir(2)-In(5)#5	2.6275(10)
Ir(2)-In(5)	2.6275(10)
Ir(2)-In(6)	2.6674(18)
Ir(3)-In(7)	2.5437(13)
Ir(3)-In(7)#7	2.5437(13)
Ir(3)-In(7)#8	2.5437(13)
Ir(3)-In(8)	2.5546(17)
Ir(3)-In(8)#8	2.5546(17)
Ir(3)-In(8)#7	2.5546(17)
Ir(3)-In(9)	2.600(6)
Ir(3)-In(9)#8	2.600(6)
Ir(3)-In(9)#7	2.600(6)
Ir(3)-In(10)	2.94(4)
In(1)-Ir(1)#9	2.6213(10)
In(1)-In(5)#9	3.2639(12)
In(1)-In(7)#10	3.2896(13)
In(1)-S(1)#6	2.605(3)
In(1)-S(3)	2.584(3)
In(1)-S(4)	2.516(2)
In(2)-Ir(1)#10	2.6155(12)
In(2)-In(5)#10	3.2403(13)
In(2)-In(5)#11	3.2403(13)
In(2)-S(2)	2.534(4)

In(2)-S(3)	2.576(3)
In(2)-S(3)#4	2.576(3)
In(3)-In(5)	3.2576(12)
In(3)-In(5)#5	3.1950(13)
In(3)-In(6)	3.3262(14)
In(3)-S(1)	2.577(3)
In(3)-S(2)#5	2.613(3)
In(3)-S(5)	2.519(4)
In(4)-In(5)	3.2876(14)
In(4)-In(5)#4	3.2876(14)
In(4)-In(7)#5	3.2126(18)
In(4)-S(1)	2.578(3)
In(4)-S(1)#4	2.578(3)
In(4)-S(2)	2.602(4)
In(5)-In(1)#1	3.2639(12)
In(5)-In(2)#3	3.2402(13)
In(5)-In(3)#6	3.1950(13)
In(6)-In(3)#5	3.3262(14)
In(6)-In(3)#6	3.3262(14)
In(6)-S(3)#5	2.680(3)
In(6)-S(3)	2.680(3)
In(6)-S(3)#6	2.680(3)
In(7)-Ir(1)#6	2.6694(13)
In(7)-In(1)#12	3.2895(13)
In(7)-In(1)#3	3.2895(13)
In(7)-In(4)#6	3.2127(18)
In(7)-In(9)	3.250(5)
In(7)-In(9)#7	3.250(5)
In(8)-S(1)#13	2.632(3)
In(8)-S(1)#6	2.632(3)
In(8)-S(4)	2.715(5)
In(8)-In(9)	0.858(8)
In(8)-In(10)	2.43(2)
S(1)-In(1)#5	2.605(3)
S(1)-In(8)#5	2.632(3)
S(1)-In(9)#5	2.614(4)

S(2)-In(3)#6	2.613(3)
S(2)-In(3)#13	2.613(3)
S(4)-In(1)#4	2.516(2)
S(4)-In(10)	2.57(2)
S(5)-In(3)#14	2.519(4)
S(5)-In(9)#5	2.865(10)
In(9)-In(7)#8	3.250(5)
In(9)-S(1)#6	2.614(4)
In(9)-S(1)#13	2.614(4)
In(9)-S(5)#6	2.865(10)
In(9)-In(10)	3.23(3)
In(10)-In(8)#8	2.43(2)
In(10)-In(8)#7	2.43(2)
In(10)-S(4)#8	2.57(2)
In(10)-S(4)#7	2.57(2)
In(10)-In(9)#7	3.23(3)
In(10)-In(9)#8	3.23(3)

Symmetry transformations used to generate equivalent atoms:
(1) -y+1,x-y+1,z+1 (2) y-1,x,z+1 (3) x,y,z+1 (4) -x,-x+y,z (5) -y+1,x-y+1,z (6) -x+y,-x+1,z (7) -y+1,x-y+2,z (8) -x+y-1,-x+1,z (9) -x+y,-x+1,z-1 (10) x,y,z-1 (11) -x,-x+y,z-1 (12) x-y+1,-y+2,z+1 (13) x-y,-y+1,z (14) y,x,z

Table S4. Bond angles [°] for $Ir_6In_{32}S_{21}$ at 299 K with estimated standard deviations in parentheses.

Label	Angles
In(1)#1-Ir(1)-In(1)#2	87.81(4)
In(1)#1-Ir(1)-In(4)	126.74(3)
In(1)#2-Ir(1)-In(4)	126.74(3)
In(1)#1-Ir(1)-In(5)#4	156.50(4)
In(1)#2-Ir(1)-In(5)	156.50(4)
In(1)#1-Ir(1)-In(5)	76.37(3)
In(1)#2-Ir(1)-In(5)#4	76.37(3)
In(1)#2-Ir(1)-In(7)#5	76.88(3)
In(1)#1-Ir(1)-In(7)#5	76.88(3)
In(2)#3-Ir(1)-In(1)#1	85.96(4)
In(2)#3-Ir(1)-In(1)#2	85.96(4)
In(2)#3-Ir(1)-In(4)	129.49(4)
In(2)#3-Ir(1)-In(5)#4	75.82(3)
In(2)#3-Ir(1)-In(5)	75.81(3)
In(2)#3-Ir(1)-In(7)#5	156.02(5)
In(4)-Ir(1)-In(5)#4	76.73(3)
In(4)-Ir(1)-In(5)	76.73(3)
In(4)-Ir(1)-In(7)#5	74.49(4)
In(5)#4-Ir(1)-In(5)	112.42(4)
In(5)-Ir(1)-In(7)#5	115.26(3)
In(5)#4-Ir(1)-In(7)#5	115.26(3)
In(3)#6-Ir(2)-In(3)#5	115.57(2)
In(3)#5-Ir(2)-In(3)	115.57(2)
In(3)#6-Ir(2)-In(3)	115.57(2)
In(3)-Ir(2)-In(6)	77.67(3)
In(3)#6-Ir(2)-In(6)	77.67(3)
In(3)#5-Ir(2)-In(6)	77.67(3)
In(5)#5-Ir(2)-In(3)#6	153.73(5)
In(5)-Ir(2)-In(3)	76.46(3)
In(5)#5-Ir(2)-In(3)	74.74(3)
In(5)#6-Ir(2)-In(3)#6	76.46(3)
In(5)#6-Ir(2)-In(3)#5	74.74(3)
In(5)#6-Ir(2)-In(3)	153.73(5)
In(5)-Ir(2)-In(3)#6	74.74(3)

In(5)#5-Ir(2)-In(3)#5	76.46(3)
In(5)-Ir(2)-In(3)#5	153.73(5)
In(5)-Ir(2)-In(5)#5	85.23(4)
In(5)#6-Ir(2)-In(5)#5	85.23(4)
In(5)#6-Ir(2)-In(5)	85.23(4)
In(5)#6-Ir(2)-In(6)	128.58(3)
In(5)#5-Ir(2)-In(6)	128.58(3)
In(5)-Ir(2)-In(6)	128.58(3)
In(7)#7-Ir(3)-In(7)	90.57(5)
In(7)#8-Ir(3)-In(7)	90.57(5)
In(7)#7-Ir(3)-In(7)#8	90.57(5)
In(7)#7-Ir(3)-In(8)	176.70(6)
In(7)#8-Ir(3)-In(8)#8	91.75(4)
In(7)#7-Ir(3)-In(8)#7	91.75(4)
In(7)#8-Ir(3)-In(8)	91.75(4)
In(7)-Ir(3)-In(8)#8	176.70(6)
In(7)-Ir(3)-In(8)	91.75(4)
In(7)#8-Ir(3)-In(8)#7	176.70(6)
In(7)#7-Ir(3)-In(8)#8	91.75(4)
In(7)-Ir(3)-In(8)#7	91.75(4)
In(7)#7-Ir(3)-In(9)	164.16(18)
In(7)#8-Ir(3)-In(9)#8	78.37(12)
In(7)#8-Ir(3)-In(9)#7	164.16(18)
In(7)#8-Ir(3)-In(9)	78.37(12)
In(7)#7-Ir(3)-In(9)#7	78.37(12)
In(7)-Ir(3)-In(9)	78.37(12)
In(7)-Ir(3)-In(9)#7	78.37(12)
In(7)#7-Ir(3)-In(9)#8	78.37(12)
In(7)-Ir(3)-In(9)#8	164.16(18)
In(7)-Ir(3)-In(10)	124.86(4)
In(7)#7-Ir(3)-In(10)	124.86(3)
In(7)#8-Ir(3)-In(10)	124.86(4)
In(8)-Ir(3)-In(8)#7	85.83(7)
In(8)-Ir(3)-In(8)#8	85.83(7)
In(8)#8-Ir(3)-In(8)#7	85.83(7)
In(8)#7-Ir(3)-In(9)#8	99.81(13)

In(8)#7-Ir(3)-In(9)#7	19.14(18)
In(8)#7-Ir(3)-In(9)	99.81(13)
In(8)#8-Ir(3)-In(9)	99.81(13)
In(8)-Ir(3)-In(9)#8	99.81(13)
In(8)-Ir(3)-In(9)#7	99.81(13)
In(8)#8-Ir(3)-In(9)#8	19.14(18)
In(8)-Ir(3)-In(9)	19.14(18)
In(8)#8-Ir(3)-In(9)#7	99.81(13)
In(8)#8-Ir(3)-In(10)	51.84(5)
In(8)#7-Ir(3)-In(10)	51.84(5)
In(8)-Ir(3)-In(10)	51.84(5)
In(9)#8-Ir(3)-In(9)#7	109.92(17)
In(9)-Ir(3)-In(9)#7	109.92(17)
In(9)-Ir(3)-In(9)#8	109.92(17)
In(9)-Ir(3)-In(10)	70.98(17)
In(9)#7-Ir(3)-In(10)	70.98(17)
In(9)#8-Ir(3)-In(10)	70.98(17)
Ir(1)#9-In(1)-In(5)#9	52.32(2)
Ir(1)#9-In(1)-In(7)#10	52.22(3)
In(5)#9-In(1)-In(7)#10	86.73(4)
S(1)#6-In(1)-Ir(1)#9	127.64(8)
S(1)#6-In(1)-In(5)#9	131.25(6)
S(1)#6-In(1)-In(7)#10	135.16(6)
S(3)-In(1)-Ir(1)#9	114.08(8)
S(3)-In(1)-In(5)#9	62.52(8)
S(3)-In(1)-In(7)#10	136.23(8)
S(3)-In(1)-S(1)#6	87.68(10)
S(4)-In(1)-Ir(1)#9	118.17(11)
S(4)-In(1)-In(5)#9	141.65(11)
S(4)-In(1)-In(7)#10	67.39(11)
S(4)-In(1)-S(1)#6	85.56(12)
S(4)-In(1)-S(3)	118.16(15)
Ir(1)#10-In(2)-In(5)#10	52.69(3)
Ir(1)#10-In(2)-In(5)#11	52.69(3)
In(5)#11-In(2)-In(5)#10	85.96(5)
S(2)-In(2)-Ir(1)#10	133.83(10)

S(2)-In(2)-In(5)#10	135.66(3)
S(2)-In(2)-In(5)#11	135.66(3)
S(2)-In(2)-S(3)	89.05(9)
S(2)-In(2)-S(3)#4	89.05(9)
S(3)-In(2)-Ir(1)#10	112.18(8)
S(3)#4-In(2)-Ir(1)#10	112.19(8)
S(3)#4-In(2)-In(5)#10	132.62(9)
S(3)#4-In(2)-In(5)#11	60.17(8)
S(3)-In(2)-In(5)#10	60.17(8)
S(3)-In(2)-In(5)#11	132.62(9)
S(3)#4-In(2)-S(3)	118.97(16)
Ir(2)-In(3)-In(5)#5	52.50(3)
Ir(2)-In(3)-In(5)	51.64(3)
Ir(2)-In(3)-In(6)	51.58(3)
In(5)#5-In(3)-In(5)	66.92(4)
In(5)#5-In(3)-In(6)	94.01(3)
In(5)-In(3)-In(6)	92.87(3)
S(1)-In(3)-Ir(2)	114.21(7)
S(1)-In(3)-In(5)#5	158.67(8)
S(1)-In(3)-In(5)	91.75(8)
S(1)-In(3)-In(6)	86.27(7)
S(1)-In(3)-S(2)#5	110.16(13)
S(2)#5-In(3)-Ir(2)	114.12(8)
S(2)#5-In(3)-In(5)#5	91.15(10)
S(2)#5-In(3)-In(5)	158.01(10)
S(2)#5-In(3)-In(6)	86.96(7)
S(5)-In(3)-Ir(2)	130.86(14)
S(5)-In(3)-In(5)#5	86.17(15)
S(5)-In(3)-In(5)	91.19(10)
S(5)-In(3)-In(6)	175.67(9)
S(5)-In(3)-S(1)	95.13(15)
S(5)-In(3)-S(2)#5	88.71(10)
Ir(1)-In(4)-In(5)#4	51.90(3)
Ir(1)-In(4)-In(5)	51.90(3)
Ir(1)-In(4)-In(7)#5	53.19(3)
In(5)-In(4)-In(5)#4	84.44(4)

In(7)#5-In(4)-In(5)#4	87.61(4)
In(7)#5-In(4)-In(5)	87.61(4)
S(1)-In(4)-Ir(1)	123.44(7)
S(1)#4-In(4)-Ir(1)	123.44(7)
S(1)-In(4)-In(5)	91.05(6)
S(1)#4-In(4)-In(5)#4	91.05(6)
S(1)-In(4)-In(5)#4	175.05(8)
S(1)#4-In(4)-In(5)	175.05(8)
S(1)#4-In(4)-In(7)#5	90.18(7)
S(1)-In(4)-In(7)#5	90.18(7)
S(1)-In(4)-S(1)#4	93.38(13)
S(1)#4-In(4)-S(2)	92.69(10)
S(1)-In(4)-S(2)	92.69(10)
S(2)-In(4)-Ir(1)	122.63(10)
S(2)-In(4)-In(5)	89.30(7)
S(2)-In(4)-In(5)#4	89.30(7)
S(2)-In(4)-In(7)#5	175.83(10)
Ir(1)-In(5)-In(1)#1	51.31(2)
Ir(1)-In(5)-In(2)#3	51.50(3)
Ir(1)-In(5)-In(3)#6	114.56(4)
Ir(1)-In(5)-In(3)	110.93(4)
Ir(1)-In(5)-In(4)	51.37(3)
Ir(2)-In(5)-Ir(1)	154.44(5)
Ir(2)-In(5)-In(1)#1	140.16(4)
Ir(2)-In(5)-In(2)#3	146.42(4)
Ir(2)-In(5)-In(3)#6	52.76(2)
Ir(2)-In(5)-In(3)	51.89(2)
Ir(2)-In(5)-In(4)	103.20(4)
In(1)#1-In(5)-In(4)	91.73(3)
In(2)#3-In(5)-In(1)#1	66.58(4)
In(2)#3-In(5)-In(3)	161.56(4)
In(2)#3-In(5)-In(4)	93.42(3)
In(3)#6-In(5)-In(1)#1	165.82(4)
In(3)-In(5)-In(1)#1	98.67(3)
In(3)#6-In(5)-In(2)#3	104.58(4)
In(3)#6-In(5)-In(3)	87.48(4)

In(3)#6-In(5)-In(4)	77.40(3)
In(3)-In(5)-In(4)	75.37(3)
Ir(2)-In(6)-In(3)	50.75(3)
Ir(2)-In(6)-In(3)#5	50.75(3)
Ir(2)-In(6)-In(3)#6	50.75(3)
Ir(2)-In(6)-S(3)#6	129.49(8)
Ir(2)-In(6)-S(3)#5	129.49(8)
Ir(2)-In(6)-S(3)	129.49(8)
In(3)#6-In(6)-In(3)#5	84.23(4)
In(3)#6-In(6)-In(3)	84.23(4)
In(3)#5-In(6)-In(3)	84.23(4)
S(3)#5-In(6)-In(3)#5	133.42(6)
S(3)#6-In(6)-In(3)	135.64(6)
S(3)#6-In(6)-In(3)#5	78.76(8)
S(3)#5-In(6)-In(3)#6	135.64(6)
S(3)#5-In(6)-In(3)	78.76(8)
S(3)-In(6)-In(3)#5	135.64(6)
S(3)-In(6)-In(3)	133.42(6)
S(3)#6-In(6)-In(3)#6	133.42(6)
S(3)-In(6)-In(3)#6	78.76(8)
S(3)-In(6)-S(3)#6	83.87(12)
S(3)-In(6)-S(3)#5	83.87(12)
S(3)#6-In(6)-S(3)#5	83.87(12)
Ir(1)#6-In(7)-In(1)#3	50.90(3)
Ir(1)#6-In(7)-In(1)#12	50.90(3)
Ir(1)#6-In(7)-In(4)#6	52.32(3)
Ir(1)#6-In(7)-In(9)	116.43(9)
Ir(1)#6-In(7)-In(9)#7	116.43(9)
Ir(3)-In(7)-Ir(1)#6	160.78(6)
Ir(3)-In(7)-In(1)#3	140.79(3)
Ir(3)-In(7)-In(1)#12	140.79(3)
Ir(3)-In(7)-In(4)#6	108.47(5)
Ir(3)-In(7)-In(9)#7	51.59(11)
Ir(3)-In(7)-In(9)	51.59(11)
In(1)#12-In(7)-In(1)#3	67.09(5)
In(4)#6-In(7)-In(1)#3	92.62(4)

In(4)#6-In(7)-In(1)#12	92.62(4)
In(4)#6-In(7)-In(9)#7	77.81(7)
In(4)#6-In(7)-In(9)	77.81(7)
In(9)-In(7)-In(1)#12	167.26(10)
In(9)#7-In(7)-In(1)#3	167.26(10)
In(9)#7-In(7)-In(1)#12	104.56(13)
In(9)-In(7)-In(1)#3	104.56(13)
In(9)-In(7)-In(9)#7	81.8(3)
Ir(3)-In(8)-S(1)#13	119.86(8)
Ir(3)-In(8)-S(1)#6	119.86(8)
Ir(3)-In(8)-S(4)	132.02(12)
S(1)#6-In(8)-S(1)#13	112.80(14)
S(1)#13-In(8)-S(4)	81.16(10)
S(1)#6-In(8)-S(4)	81.16(10)
In(9)-In(8)-Ir(3)	83.4(4)
In(9)-In(8)-S(1)#13	79.4(2)
In(9)-In(8)-S(1)#6	79.4(2)
In(9)-In(8)-S(4)	144.5(4)
In(9)-In(8)-In(10)	155.7(10)
In(10)-In(8)-Ir(3)	72.3(8)
In(10)-In(8)-S(1)#13	112.4(4)
In(10)-In(8)-S(1)#6	112.4(4)
In(10)-In(8)-S(4)	59.7(8)
In(1)#5-S(1)-In(8)#5	96.42(10)
In(1)#5-S(1)-In(9)#5	113.32(19)
In(3)-S(1)-In(1)#5	120.40(11)
In(3)-S(1)-In(4)	101.82(10)
In(3)-S(1)-In(8)#5	106.57(12)
In(3)-S(1)-In(9)#5	90.16(19)
In(4)-S(1)-In(1)#5	122.52(12)
In(4)-S(1)-In(8)#5	107.53(10)
In(4)-S(1)-In(9)#5	102.84(15)
In(9)#5-S(1)-In(8)#5	18.83(17)
In(2)-S(2)-In(3)#6	120.59(11)
In(2)-S(2)-In(3)#13	120.59(11)
In(2)-S(2)-In(4)	118.29(15)

In(3)#6-S(2)-In(3)#13	87.72(12)
In(4)-S(2)-In(3)#13	102.03(12)
In(4)-S(2)-In(3)#6	102.03(12)
In(1)-S(3)-In(6)	113.03(11)
In(2)-S(3)-In(1)	120.31(15)
In(2)-S(3)-In(6)	112.06(11)
In(1)-S(4)-In(1)#4	122.9(2)
In(1)#4-S(4)-In(8)	96.49(12)
In(1)-S(4)-In(8)	96.49(12)
In(1)-S(4)-In(10)	116.33(19)
In(1)#4-S(4)-In(10)	116.33(19)
In(10)-S(4)-In(8)	54.5(8)
In(3)-S(5)-In(3)#14	91.91(17)
In(3)#14-S(5)-In(9)#5	85.88(19)
In(3)-S(5)-In(9)#5	85.88(19)
Ir(3)-In(9)-In(7)	50.04(10)
Ir(3)-In(9)-In(7)#8	50.04(10)
Ir(3)-In(9)-S(1)#6	118.79(15)
Ir(3)-In(9)-S(1)#13	118.79(15)
Ir(3)-In(9)-S(5)#6	124.2(3)
Ir(3)-In(9)-In(10)	59.4(6)
In(7)#8-In(9)-In(7)	67.57(13)
In(8)-In(9)-Ir(3)	77.4(4)
In(8)-In(9)-In(7)	112.0(4)
In(8)-In(9)-In(7)#8	112.0(4)
In(8)-In(9)-S(1)#13	81.7(3)
In(8)-In(9)-S(1)#6	81.7(3)
In(8)-In(9)-S(5)#6	158.4(5)
In(8)-In(9)-In(10)	18.0(7)
S(1)#6-In(9)-In(7)#8	155.5(2)
S(1)#6-In(9)-In(7)	88.72(10)
S(1)#13-In(9)-In(7)	155.5(2)
S(1)#13-In(9)-In(7)#8	88.72(9)
S(1)#6-In(9)-S(1)#13	113.9(3)
S(1)#13-In(9)-S(5)#6	86.58(18)
S(1)#6-In(9)-S(5)#6	86.58(18)

S(1)#6-In(9)-In(10)	91.5(4)
S(1)#13-In(9)-In(10)	91.5(4)
S(5)#6-In(9)-In(7)	85.66(19)
S(5)#6-In(9)-In(7)#8	85.66(19)
S(5)#6-In(9)-In(10)	176.4(6)
In(10)-In(9)-In(7)#8	97.3(5)
In(10)-In(9)-In(7)	97.3(5)
Ir(3)-In(10)-In(9)	49.6(6)
Ir(3)-In(10)-In(9)#8	49.6(6)
Ir(3)-In(10)-In(9)#7	49.6(6)
In(8)#8-In(10)-Ir(3)	55.9(8)
In(8)#7-In(10)-Ir(3)	55.9(8)
In(8)-In(10)-Ir(3)	55.9(8)
In(8)-In(10)-In(8)#8	91.6(12)
In(8)-In(10)-In(8)#7	91.6(12)
In(8)#7-In(10)-In(8)#8	91.6(12)
In(8)-In(10)-S(4)	65.72(12)
In(8)#7-In(10)-S(4)#8	130.28(7)
In(8)#8-In(10)-S(4)#8	65.72(12)
In(8)#7-In(10)-S(4)	130.28(8)
In(8)#8-In(10)-S(4)#7	130.28(7)
In(8)#8-In(10)-S(4)	130.28(8)
In(8)-In(10)-S(4)#7	130.28(7)
In(8)-In(10)-S(4)#8	130.28(8)
In(8)#7-In(10)-S(4)#7	65.72(12)
In(8)-In(10)-In(9)	6.3(3)
In(8)#8-In(10)-In(9)#7	87.2(10)
In(8)-In(10)-In(9)#8	87.2(10)
In(8)#7-In(10)-In(9)	87.2(10)
In(8)#8-In(10)-In(9)#8	6.3(3)
In(8)-In(10)-In(9)#7	87.2(10)
In(8)#7-In(10)-In(9)#8	87.2(10)
In(8)#7-In(10)-In(9)#7	6.3(3)
In(8)#8-In(10)-In(9)	87.2(10)
S(4)#8-In(10)-Ir(3)	121.6(8)
S(4)#7-In(10)-Ir(3)	121.6(8)

S(4)-In(10)-Ir(3)	121.6(8)
S(4)#8-In(10)-S(4)#7	95.1(11)
S(4)#8-In(10)-S(4)	95.1(11)
S(4)#7-In(10)-S(4)	95.1(11)
S(4)#8-In(10)-In(9)#7	131.6(3)
S(4)-In(10)-In(9)#7	131.6(3)
S(4)#8-In(10)-In(9)#8	72.0(3)
S(4)-In(10)-In(9)#8	131.6(3)
S(4)#7-In(10)-In(9)#8	131.6(3)
S(4)#8-In(10)-In(9)	131.6(3)
S(4)#7-In(10)-In(9)#7	72.0(3)
S(4)#7-In(10)-In(9)	131.6(3)
S(4)-In(10)-In(9)	72.0(3)
In(9)#7-In(10)-In(9)#8	82.5(9)
In(9)-In(10)-In(9)#7	82.5(9)
In(9)-In(10)-In(9)#8	82.5(9)

Symmetry transformations used to generate equivalent atoms:
(1) -y+1,x-y+1,z+1 (2) y-1,x,z+1 (3) x,y,z+1 (4) -x,-x+y,z (5) -y+1,x-y+1,z (6) -x+y,-x+1,z (7) -y+1,x-y+2,z (8) -x+y-1,-x+1,z (9) -x+y,-x+1,z-1 (10) x,y,z-1 (11) -x,-x+y,z-1 (12) x-y+1,-y+2,z+1 (13) x-y,-y+1,z (14) y,x,z

References:

1. S. A. Denev, T. T. A. Lummen, E. Barnes, A. Kumar and V. Gopalan, *J. Am. Ceram. Soc.*, 2011, **94**, 2699-2727.
2. S. Lei, M. Gu, D. Puggioni, G. Stone, J. Peng, J. Ge, Y. Wang, B. Wang, Y. Yuan, K. Wang, Z. Mao, J. M. Rondinelli and V. Gopalan, *Nano Lett.*, 2018, **18**, 3088-3095.